

Final Draft
of the original manuscript:

Matthias, V.; Aulinger, A.; Bieser, J.; Cuesta, J.; Geyer, B.; Langmann, B.;
Serikov, I.; Mattis, I.; Minikin, A.; Mona, L.; Quante, M.; Schumann, U.;
Weinzierl, B.:

**The ash dispersion over Europe during the Eyjafjallajökull
eruption – Comparison of CMAQ simulations to remote sensing
and air-borne in-situ observations**

In: Atmospheric Environment (2011) Elsevier

DOI: 10.1016/j.atmosenv.2011.06.077

The ash dispersion over Europe during the Eyjafjallajökull eruption - comparison of CMAQ simulations to remote sensing and in-situ observations

Volker Matthias^{a,*}, Armin Aulinger^a, Johannes Bieser^a, Juan Cuesta^{b,c}, Beate Geyer^a, Bärbel Langmann^e, Ilya Serikov^f, Ina Mattis^g, Andreas Minikin^h, Lucia Mona^d, Markus Quante^a, Ulrich Schumann^h, Bernadett Weinzierl^h

^a*Helmholtz-Zentrum Geesthacht, Institute of Coastal Research, Max-Planck-Straße 1, 21502 Geesthacht, Germany*

^b*Laboratoire Inter-Universitaire des Systèmes Atmosphériques (LISA), Université Paris Est Créteil (UPEC) 61, Avenue du Général de Gaulle, 94010 Créteil Cedex, France*

^c*Laboratoire Atmospheres Milieux Observations Spatiales (LATMOS), 4 Place Jussieu, 75252 Paris, France*

^d*CNR-IMAA, C.da S. Loja, I-85050 Tito Scalo, Potenza, Italy*

^e*Institute of Geophysics, University of Hamburg, KlimaCampus, Bundesstraße 55, 20146 Hamburg, Germany*

^f*Max-Planck-Institut für Meteorologie, Bundesstraße 55, 20146 Hamburg, Germany*

^g*Leibniz Institute for Tropospheric Research, Permoserstrasse 15, 04318 Leipzig, Germany*

^h*Deutsches Zentrum für Luft- und Raumfahrt (DLR), Institut für Physik der Atmosphäre, Münchner Straße 20, 82230 Oberpfaffenhofen, Germany*

Abstract

The dispersion of volcanic ash over Europe after the outbreak of the Eyjafjallajökull on Iceland on 14 April 2010 has been simulated with a conventional three-dimensional Eulerian chemistry transport model system, the Community Multiscale Air Quality (CMAQ) model. Four different emission scenarios representing the lower and upper bounds of the emission height and intensity were considered. The atmospheric ash concentrations turned out to be highly variable in time and space. The model results were compared to three different kinds of ob-

*corresponding author, Phone +49-4152-872346, Fax + 49-4152-872332
Email address: volker.matthias@hzg.de (Volker Matthias)

servations: Aeronet aerosol optical depth (AOD) measurements, Earlinet aerosol extinction profiles and in-situ observations of the ash concentration by means of optical particle counters aboard the DLR Falcon aircraft. The model was able to reproduce observed AOD values and atmospheric ash concentrations. Best agreement was achieved for lower emission heights and a fraction of 2 % transportable ash in the total volcanic emissions. The complex vertical structure of the volcanic ash layers in the free troposphere could not be simulated. Compared to the observations, the model tends to show vertically more extended, homogeneous aerosol layers.

Keywords: volcanic eruption, ash dispersion, chemistry transport model, lidar, sun photometer, ash concentration

1. Introduction

Volcanoes are the by far largest point sources on Earth that emit particles (ash) and gases, in particular sulphur dioxide into the atmosphere. Their emission strength is highly variable in time. Typically high emissions take place for only few days or weeks while they are very low most of the time. High volcanic ash concentrations in the atmosphere lead to low visibility, reduced solar radiation reaching the surface and might cause negative health effects for people who were exposed to high ash concentrations in air. Most of these effects are quite local, only very huge eruptions that emit particles and sulphur dioxide directly into the stratosphere may have long lasting effects on the solar radiation and thus on climate.

During the eruption of the Icelandic volcano Eyjafjallajökull between 14 April and 22 May 2010 the volcanic ash was transported into regions with high air traf-

14 fic density. This was particularly the case in the beginning of the eruption phase
15 when strong northwesterly winds transported high amounts of aerosol particles to
16 Central Europe. The air space over Europe was almost completely closed between
17 16 April and 21 April 2010 causing high losses for the airlines. Also other indus-
18 tries that rely on the timely delivery of necessary components faced problems to
19 maintain their production. Numerous air passengers were stuck at the airports and
20 could not reach their destination. In the following the airlines claimed that the
21 grounding of the aircrafts was not justified because the ash concentrations were
22 low and would not cause any damage to the turbines of their jets. However, it
23 was not clear how high the ash concentrations were and neither the Volcanic Ash
24 Advisory Center (VAAC) that is responsible for the calculation of the ash disper-
25 sion by means of atmospheric models, nor any other institution could give reliable
26 numbers of the aerosol concentration and the altitude of the aerosol layers in the
27 free troposphere.

28 Three-dimensional dynamical numerical models can help to get a more compre-
29 hensive picture of the ash distribution in the atmosphere after a volcanic eruption.
30 Chemistry transport models are capable of simulating the transport of small parti-
31 cles in the atmosphere provided the necessary input parameters are at hand. These
32 are accurate three dimensional meteorological and emission fields. Meteorolog-
33 ical fields can be simulated with mesoscale models which are driven by global
34 reanalysis data that is available shortly after atmospheric observations have been
35 reported. The models can also be applied in forecast mode giving the possibility
36 to calculate the ash distribution in real time or to forecast the development of the
37 ash cloud. The largest uncertainties are connected with the emission strength and
38 the altitudes up to which the ash is emitted by the volcanic eruption. It is possible

39 to estimate the emission heights by visual inspection or by radar observations in
40 the vicinity of the volcano, the amount of the emitted ash can then be assessed by
41 simple empirical relations between emission height and emission intensity. Only
42 a minor part of the emitted particles are small enough that they may be transported
43 over several thousands of kilometers in the upper troposphere. This size fraction
44 is again subject to large uncertainties. Therefore it is highly recommendable to
45 compare the results of the ash transport simulations to all observations that are
46 available to assess the uncertainties connected with the emissions that feed the
47 simulation. If this can be assured, the simulations can be used to give an estimate
48 about the distribution of the ash concentrations in the atmosphere in space and
49 time.

50 This paper describes simulations of the ash transport of the Eyjafjallajökull vol-
51 canic eruption between 14 April and 22 May 2010. The calculations have been
52 done with a conventional Eulerian chemistry transport model, the Community
53 Multiscale Air Quality (CMAQ) model. The model system together with its input
54 parameters is described in section 2 of this paper. The capability of the model sys-
55 tem to give a comprehensive picture of the ash distribution over Europe has been
56 tested. The observational data that was compared to the model results includes
57 sun photometer measurements, lidar profiles and in-situ observations of the ash
58 concentrations aboard an aircraft. It is described in section 3 while the simulation
59 results and their comparison to the observations are discussed in section 4.

60 **2. Model description**

61 *2.1. Chemistry transport model*

62 CMAQ has originally been developed to study air pollution episodes, in partic-
63 ular ozone episodes, in the United States. It has been further developed in recent
64 years to simulate pollution by aerosol particles, heavy metals and mercury but it
65 has not been built or adapted to treat especially volcanic ash transport in high al-
66 titudes. The model includes gas phase, aerosol and aqueous chemistry, primary
67 and secondary particles and it is widely used to simulate atmospheric transport of
68 particles. It should therefore in principle be suited to treat volcanic ash transport,
69 too. In this study, the CBM4 chemical mechanism (Gery et al., 1989) is used.
70 The aerosol is represented by 11 different classes and three size modes (Aitken,
71 accumulation and coarse mode). Each of them is assumed to have a lognormal
72 distribution. Volcanic ash is best represented by coarse mode aerosol particles. In
73 CMAQ they have a geometric mean diameter of $6 \mu\text{m}$, the standard deviation of
74 the logarithm of the particle size is 2.2.

75 For our study the CMAQ model was set up on a $24 \times 24 \text{ km}^2$ grid for Northwest
76 Europe. This model domain was nested into a larger $72 \times 72 \text{ km}^2$ grid covering
77 Europe and parts of North Africa. Thirty vertical levels up to 20 hPa with 20 lev-
78 els below approx. 2500 m were used in a terrain following σ -pressure co-ordinate
79 system. In the vertical, this is the standard setup of the model as it has been used
80 for simulations of the aerosol distribution and benzo(a)pyrene concentrations in
81 Europe (Matthias, 2008; Matthias et al., 2009).

82 2.2. Emissions

83 The emissions of the Eyjafjallajökull volcano were estimated based on an em-
84 pirical relationship between plume height and the eruption volume rate given by
85 Mastin et al. (2009). Both emission heights and resulting tephra flux are pre-
86 sented in the introductory paper to this special issue (Langmann et al., 2011). The
87 uncertainty range has been considered by performing four model runs that are
88 defined by the upper and lower limits of the emission heights (called MIN and
89 MAX emission cases) and the upper and lower limits of the fraction of trans-
90 portable ash related to the total tephra emissions. Measured grain size dis-
91 tributions close to Eyjafjallajökull (http://www.earthice.hi.is/page/ies_EYJO2010_Grain) show mass contributions from about 1 to 4 % for PM10
92 during the first eruption phase. Here, because also particles larger than 10 μm
93 were considered, the lower limit was assumed to be 2 % of the total tephra emis-
94 sions (MIN2 and MAX2 emissions), the upper limit to be 4 % of the total tephra
95 emissions (MIN4 and MAX4 emissions). Times series of the emission height and
96 emission strength are shown in Fig. 1. It has been assumed that volcanic ash is
97 emitted into all heights between the altitude of the volcano and the estimated max-
98 imum emission height with largest emissions in the uppermost altitudes (Fig. 1c).
99 The total emissions between 14 April and 22 May 2010 considered as coarse mode
100 aerosol are 15 and 30 Tg for the MIN2 and MIN4 cases and 25.5 and 51 Tg for
101 the MAX2 and MAX4 cases. These numbers are well within the range of 2 - 50
102 Tg (best estimate 10 Tg) derived by Schumann et al. (2010) based on airborne
103 observations close to the volcano
104

105 Emissions from anthropogenic sources as well as biogenic emissions were
106 also taken into account in the model simulations. Their consideration allows for a

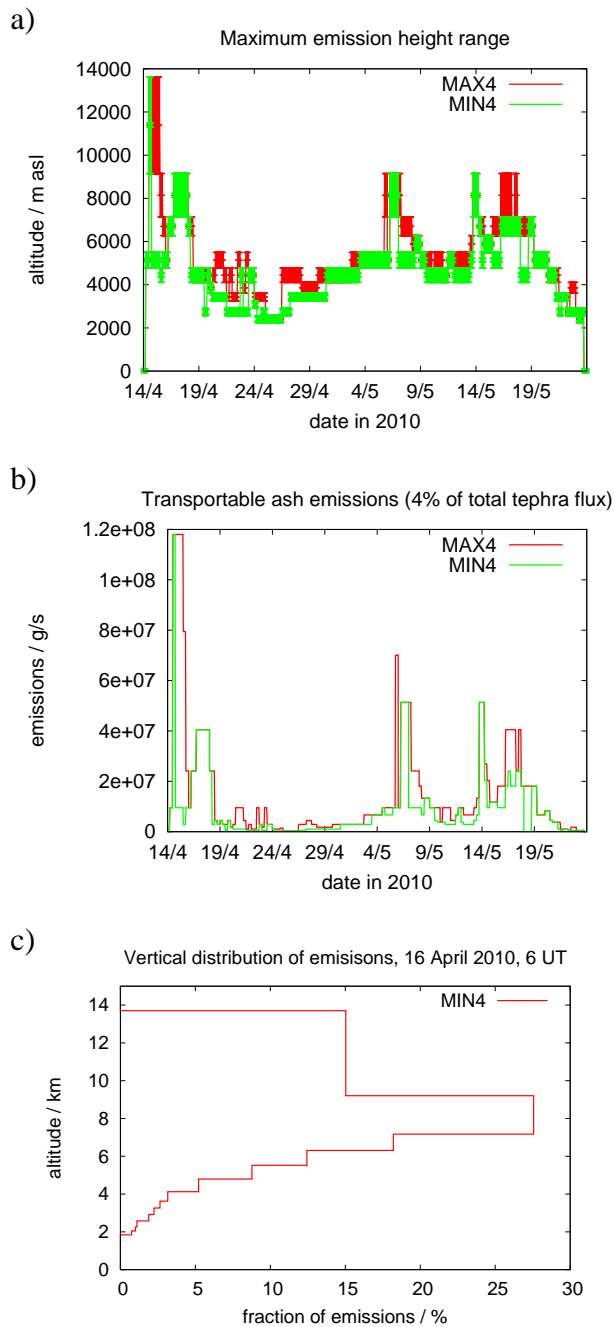


Figure 1: Volcanic emissions as described in Langmann et al. (2011): a) maximum emission heights b) total transportable ash emissions for the MIN4 and MAX4 cases and c) vertical distribution of the MIN4 emissions on 16 April 2010, 6 UT. The colored area in a) denotes the extension of the vertical layer. The MIN2 and MAX2 cases exhibit half of the emissions of the MIN4 and MAX4 cases, respectively, but in the same height intervals.

107 better comparison of the model results to ground based sun photometer observa-
108 tions. Anthropogenic emissions are based on EMEP and EPER emissions reports
109 and have been processed using the emission model SMOKE for Europe (Bieser
110 et al., 2010), biogenic emissions depend on land use (e.g. tree species), solar radi-
111 ation and temperature. They are calculated based on Guenther et al. (1995) in the
112 SMOKE for Europe emission model. Sea salt is parameterized in CMAQ using a
113 wind speed dependent approach.

114 *2.3. Initial and boundary conditions for CMAQ*

115 CMAQ was run on a $72 \times 72 \text{ km}^2$ grid for the entire European continent. The
116 results of this model run served as boundary conditions for the inner $24 \times 24 \text{ km}^2$
117 grid. By this it could be guaranteed that aerosol particles that are transported out of
118 the inner domain are not lost but may be re-advected through the boundaries. The
119 boundary conditions for the outer grid were constant at all borders. Climatological
120 vertical profiles were used for CO, O₃, NO₂, NO, HNO₃, SO₂, SO₄, PAN, NH₃,
121 and formaldehyde.

122 *2.4. Meteorological Fields*

123 The meteorological fields were derived from a simulation with the regional
124 non-hydrostatic atmospheric circulation model COSMO-CLM 4.8 (Rockel et al.,
125 2008). The simulation area covers Europe including the Mediterranean Sea to the
126 south and most part of Greenland to the northwest. The model was run with a
127 spatial resolution of $0.22^\circ \times 0.22^\circ$ and 40 vertical levels were used within a terrain
128 following coordinate system. The height of the uppermost level is about 27 km,
129 the lowest level is about 20 m above ground. The simulation is driven by NCEP-1

130 6-hourly global reanalysis data (Kalnay et al., 1996) on a $1.875^\circ \times 1.875^\circ$ grid, the
131 output interval is 1 hour.

132 **3. Measurement data**

133 *3.1. Sunphotometer*

134 The optical properties of aerosol particles in the entire atmospheric column are
135 routinely observed within the Aerosol Robotic Network (Aeronet) (Holben et al.,
136 1998). The network has grown to more than 200 stations world wide since the late
137 1990s and supplies a good continental coverage within Europe. The instruments
138 can only deliver data during daytime and during totally cloud free periods, because
139 they rely on extinction measurements of the direct and scattered solar radiation.
140 The typical uncertainty in the measured aerosol optical depth (AOD) is 0.01 to
141 0.02 (Eck et al., 1999; Holben et al., 2001). The data is submitted once a day via
142 satellite or internet to the NASA data base in Greenbelt/Maryland, USA. It can be
143 accessed via the Aeronet web page (<http://aeronet.gsfc.nasa.gov>) and is typically
144 available the day after the observations have been made. A cloud screening of
145 the measurements is done automatically shortly after the data submission. The
146 result is called level 1.5 data. It can already be used for comparisons to other
147 observations or to modelled AOD data. The final quality control is done after
148 another calibration of the instruments which is done once a year. Afterwards the
149 highest level 2 of the data quality is reached.

150 Besides the most important information about the AOD, other data products might
151 be available, depending on cloud amount and the AOD value. During the eruption
152 of the Eyjafjallajökull, the sky over Central Europe was cloud-free for many days.
153 Therefore it was possible to derive a size dependent aerosol optical depth. This

Table 1: Location and altitude of the Aeronet stations used for a comparison of AOD.

Code	Country	Station name	Latitude North	Longitude East	Altitude / m
BEL	Poland	Belsk	51.84	20.79	190
CAB	The Netherlands	Cabauw	51.97	4.92	-1
CHI	United Kingdom	Chilbolton	51.14	-1.44	88
HAM	Germany	Hamburg	53.57	9.97	105
HEL	Germany	Helgoland	54.18	7.88	33
LEI	Germany	Leipzig	51.35	12.43	125
LIL	France	Lille	50.62	3.15	60
MIN	Belarus	Minsk	53.92	27.60	200
MUN	Germany	Munich	48.15	11.57	533
PAL	France	Palaiseau	48.70	2.21	156
WYW	United Kingdom	Wytham Woods	51.77	-1.33	160

154 allowed for a detection of days when the total AOD was influenced by volcanic
 155 ash. A comparison of the modelled AOD to the Aeronet observations was done
 156 for a number of selected stations in Central and Northern Europe. An overview of
 157 these stations is given in Table 1.

158 3.2. Lidar

159 Lidar instruments are ideally suited to observe aerosol layers in higher alti-
 160 tudes. The quantity that is primarily observed is the aerosol backscatter coefficient
 161 at one or more wavelengths between the UV and the infrared. They can give in-
 162 formation about the vertical extent of the aerosol layer and about its development
 163 in time. They can be operated during day and night time. Many instruments have

Table 2: Lidar data used for comparisons to model data.

Station name	Country	Latitude North	Longitude East	Time window / UT	Quantity
Hamburg	Germany	53.57	9.97	16 April 2010, 5:30 - 5:57	extinction at 532 nm
Leipzig	Germany	51.35	12.43	16 April 2010, 12:34 - 17:00	backscatter at 532 nm
Palaiseau	France	48.7	2.21	18 April 2010, 2:30 - 3:30	backscatter at 532 nm
Potenza	Italy	40.60	15.72	20 April 2010, 22:00 - 22:30	backscatter at 532 nm

164 the capability to determine aerosol extinction and backscatter simultaneously at
 165 nighttime using the detection of Raman scattered light. This allows for the deter-
 166 mination of the extinction to backscatter ratio (so called lidar ratio), which con-
 167 tains information about the microphysical properties of the aerosol. Assuming the
 168 lidar ratio doesn't change rapidly in time, the values observed at nighttime may
 169 be used to calculate fairly reliable extinction profiles also at daytime.

170 The lidar observations used in this study were derived in the framework of the Eu-
 171 ropean Aerosol Research Lidar Network (Earlinet) (Bösenberg et al., 2003) that
 172 was established in 2000. Regular lidar observations at 27 stations in Europe are
 173 performed within this network. The data needs careful evaluation and is therefore
 174 not quickly available but it can be used upon request. Here, lidar observations at
 175 Hamburg, Leipzig, Palaiseau and Potenza are compared to model results. Details
 176 are summarized in Table 2.

177 3.3. *In-situ aircraft observations*

178 Several research flights have been undertaken with the DLR Falcon aircraft
 179 during the Eyjafjallajökull eruption to observe the ash cloud and to determine

180 its microphysical, optical and chemical properties (Schumann et al., 2010). This
181 included lidar observations from above the ash cloud, optical observations of
182 the size spectrum within the cloud and the collection of ash samples on filters
183 that could be analyzed in the laboratory. The observations of the size spectrum
184 also allowed for an estimate of the aerosol mass concentrations. This quantity
185 is directly comparable to the model results. Depending on the refractive index
186 of the scattering ash particles, the derived aerosol mass concentrations may be
187 connected with some uncertainties. A detailed discussion about the error margins
188 was done by Schumann et al. (2010). Here we compare our model concentration
189 results to the revised mass concentrations.

190

191 **4. Model results**

192 The model has been run for the period from 2 April 2010 until 23 May
193 2010. The model runs included anthropogenic emissions in order to facilitate
194 comparisons of the total optical depth to the model results. The first 12 days up
195 to 14 April, the day of the main eruption of the Eyjafjallaökull volcano, were
196 calculated to produce aerosol concentration fields that are almost independent
197 from the initial conditions. For the following period from 14 April until 23 May,
198 four runs with different assumptions about the rate and height of the volcanic
199 emissions were performed (see section 2.2).

200

201 *4.1. Ash dispersion*

202 The initial volcanic ash emissions were transported eastwards and reached the
203 Norwegian coast in the morning of 15 April. After a turn in wind direction to

204 Northwest in the evening of 14 April, the volcanic ash was rapidly transported
205 in a rather narrow corridor via the North Sea to Denmark and Northern Germany
206 where it arrived in the evening of 15 April (Fig. 2a). It was then transported south-
207 wards and was located over South Germany, large parts of France and the Benelux
208 countries on 16 and 17 April where it resided approximately until 19 April (Fig.
209 2b). Steady winds from North and Northwest over Iceland and the North Sea
210 favoured a continued transport of ash particles towards Central Europe until 20
211 April. Afterwards the emissions were lower and with changing wind directions,
212 only small amounts of ash were transported to the European continent until the
213 beginning of May. Between 2 and 5 May the United Kingdom was largely influ-
214 enced by stronger emissions in this second phase of the eruption (Fig. 2c and d).
215 In the following, large amounts of ash particles were first transported southwards
216 and then eastwards influencing mainly the Mediterranean region. Parts of the ash
217 entered again Central Europe from the Southwest on 8 and 9 May. During the last
218 stronger eruption phase between 14 and 18 May volcanic ash was like in the be-
219 ginning of the eruption transported southeastwards and reached the UK the same
220 day while the ash was located over Germany and France between 16 and 18 May
221 (Fig. 2e and f).

222 The modelled ash dispersion has been compared to forecasts provided by the Vol-
223 canic Ash Advisory Center (VAAC) in London. The VAAC uses the Lagrangian
224 NAME model to simulate the transport and the distribution of volcanic emissions
225 (Witham et al., 2007). They use standard release rates and define the borders of
226 the modelled ash cloud from a visual ash-cloud look-up table provided by NOAA.
227 Hazardous ash concentration are determined as a function of the plume height, but
228 no concentration values were given in the forecasts in April 2010. Figure 3 ex-

229 emplarilly shows the ash distribution on 17 April 2010 at 18 UT. The VAAC map
 230 is a forecast of the ash distribution in three different height ranges (0 - 20000 ft,
 231 20000 - 35000 ft, and 35000 - 55000 ft) published 6 hours before 18 UT while
 232 the CMAQ model result shows the integrated ash concentration between 2000 and
 233 13000 m asl for the emission scenario MIN2. It can be seen that both models give
 234 the same overall picture. Even a rather complex pattern of the ash distribution
 235 with some smaller ash free regions over the North Sea and some small tongues of
 236 ash reaching France and North Ireland are displayed in both model results.

237

238 4.2. Optical depth

239 In order to compare the model results to observations at several locations in
 240 Europe, the modelled atmospheric aerosol concentrations in the entire troposphere
 241 have been converted into aerosol optical depth values. A rather simple approach
 242 proposed by Malm et al. (1994) is used to calculate the aerosol extinction in the
 243 mid-visible spectrum around 500 nm wavelength. The extinction coefficient de-
 244 pends on aerosol mass and humidity in the following way:

$$\alpha_{ext} = 0.003f(RH)(m_{\text{NH}_4} + m_{\text{NO}_3} + m_{\text{SO}_4}) + 0.004 m_{\text{OM}} + \quad (1)$$

$$0.01 m_{\text{EC}} + 0.001 m_{\text{PM}_{2.5_{\text{oth}}}} + 0.0006 m_{\text{PM}_{\text{coarse}}},$$

245 where m_X denotes the mass m of species X which are ammonium (NH_4), nitrate
 246 (NO_3), sulfate (SO_4), organic matter (OM), elemental carbon (EC), other accu-
 247 mulation mode aerosols ($\text{PM}_{2.5_{\text{oth}}}$) and all coarse mode aerosol ($\text{PM}_{\text{coarse}}$). The
 248 relative humidity correction $f(RH)$ is described by Malm et al. (1994) and it is
 249 provided in look-up tables. It varies between 1 (at low RH) and 21 (at RH=99%).
 250 All coefficients in Eq. 1 are given in m^2/mg . The extinction is calculated from the

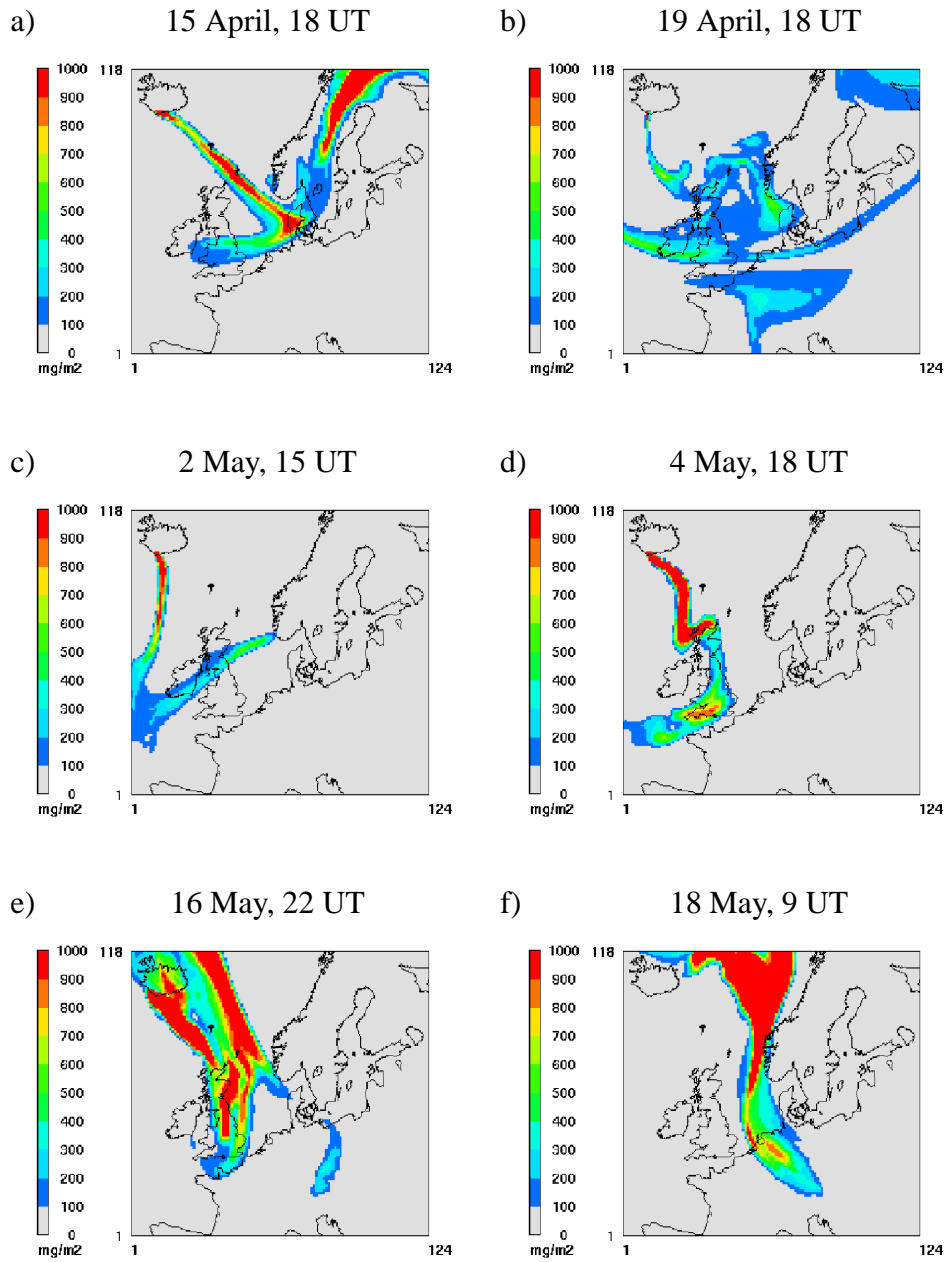


Figure 2: Temporal development of the ash cloud over Europe between 15 April and 18 May 2010 as reproduced with the CMAQ model. Given is the total ash column above 2000m for the MIN2 emission case.

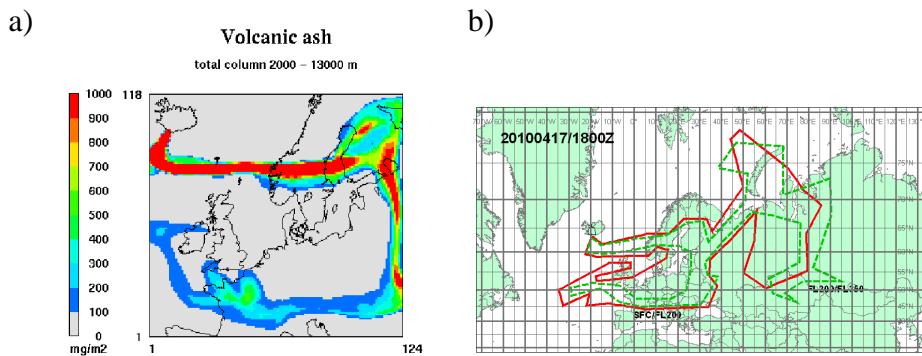


Figure 3: Comparison of a) CMAQ model results to b) a forecast provided by the Volcanic Ash Advisory Center (VAAC) on 17 April 2010, 18 UT over Central Europe.

251 aerosol mass for all model layers and then vertically integrated to give the aerosol
 252 optical depth. The method has been tested by comparing modelled aerosol optical
 253 depth values to Aeronet sun photometer observations (Matthias, 2008). It turned
 254 out that the AOD is typically underestimated by about 0.1 in the planetary bound-
 255 ary layer (PBL) but the main reason for this is the underestimation of the aerosol
 256 mass which is in the range of about 40 %. This is caused by missing organic
 257 aerosols and by too low aerosol mass in the coarse mode.

258 Because the volcanic ash is treated as coarse mode aerosol in the model there is
 259 no increase of the extinction by volcanic ash due to humidity growth. This is rea-
 260 sonable considering that the ash consists mainly of silica, aluminium oxide, iron
 261 oxide and other non-hygroscopic material and the ash plumes were often rather
 262 dry (Schumann et al., 2010).

263 Examples of the modelled and observed aerosol optical depth at four different
 264 stations (Hamburg, Chilbolton, Palaiseau and Leipzig) in the first phase of the
 265 eruption (14 - 21 April 2010) are shown in Figure 4. All emission scenarios have
 266 been considered for the comparison. The MAX4 emissions lead to very high opti-

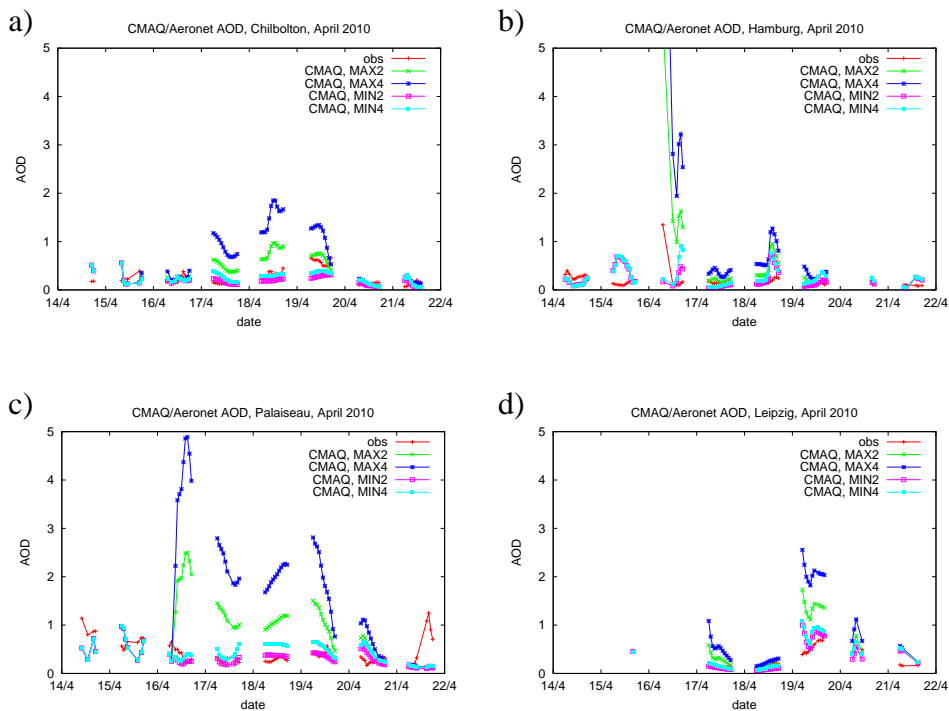


Figure 4: Comparison of CMAQ model results to Aeronet aerosol optical depth (AOD) observations between 14 and 22 April 2010 over a) Chilbolton, b) Hamburg, c) Palaiseau, and d) Leipzig.

267 cal depth values of more than 2 on several days. Such high AOD values were not
 268 observed throughout the whole period. On many days the MAX2 emissions result
 269 in too high AODs, too. The AODs calculated with the MIN2 emission values are
 270 closest to the observations at most of the stations, the MIN4 emissions still result
 271 in too high modelled AODs.

272 A statistical evaluation for all eleven stations listed in Table 3 between 16 and 21
 273 April reveals the lowest mean differences and the lowest root mean square (rms)
 274 error for the MIN2 emission scenario. The AOD caused by the volcanic ash cloud
 275 is in the same order of magnitude as the AOD caused by aerosol particles in the

Table 3: Comparison of modelled (four emission cases) and observed AOD at 11 selected Aeronet stations between 16 April and 21 April 2010. Given are the mean difference to the observations and the root mean square error. The data sets contain between 28 and 57 values.

Station	MIN2		MIN4		MAX2		MAX4	
	mean diff	rms	mean diff	rms	mean diff	rms	mean diff	rms
BEL	0.13	0.3	0.21	0.49	0.32	0.51	0.6	0.94
CAB	0.0	0.09	0.08	0.13	0.28	0.39	0.65	0.83
CHI	-0.09	0.16	-0.02	0.13	0.19	0.29	0.53	0.72
HAM	0.02	0.24	0.10	0.30	0.37	0.81	0.81	1.77
HEL	-0.09	0.23	0.0	0.29	0.44	1.17	1.05	2.53
LEI	0.02	0.15	0.08	0.19	0.28	0.46	0.61	0.86
LIL	-0.03	0.10	0.10	0.14	0.29	0.37	0.74	0.92
MIN	-0.14	0.48	-0.08	0.53	-0.01	0.54	0.17	0.76
MUN	-0.12	0.16	-0.03	0.11	0.21	0.33	0.62	0.82
PAL	-0.01	0.13	0.13	0.23	0.76	0.95	1.67	2.04
WYW	-0.08	0.18	-0.02	0.16	0.2	0.37	0.54	0.81

276 PBL. Keeping this and the fact that the AOD in the PBL is typically underesti-
277 mated by the model results in mind, the MIN2 volcanic emissions might even be
278 too high. However, the conversion from aerosol mass into extinction as described
279 in Eq. 1 also bears some uncertainties in the mass-to-extinction coefficient. Ans-
280 mann et al. (2010) used a conversion factor of 0.00051 mg/m^2 which would result
281 in approx. 15 % lower optical depth values for the same aerosol mass density. This
282 would support the fact that the emitted transportable ash is somewhere between
283 the estimates given by the MIN2 and the MIN4 scenarios.

284 4.3. Vertical profiles

285 The modelled aerosol extinction profiles at visible wavelengths has been de-
286 rived following Eq. 1. They have been compared to observed aerosol extinction
287 profiles at 532 nm which were either directly observed with the Raman Lidar
288 technique (Ansmann et al., 1992) or deduced by multiplying the aerosol backscat-
289 ter values with the lidar ratio used in the data evaluation (Fernald et al., 1972). If
290 available, this value has been taken from Raman lidar measurements during night-
291 time. At Leipzig the lidar ratio was 55 sr, at Palaiseau and Potenza a value of 50 sr
292 was taken. The results for 16 April in Hamburg and Leipzig are shown in Figure
293 5. The ash cloud reached Hamburg in the morning of 16 April, approximately
294 48 hours after the outbreak of the volcano started. At this time the highest opti-
295 cal depth values of more than 1 were observed by sunphotometers at Helgoland
296 and Hamburg (see section 4.2). The modelled profiles have been plotted for all 4
297 emission scenarios at 6 UT. The highest extinction peak that has been observed
298 by the lidar in 2800 m cannot be reproduced by the model. On the other hand
299 the modelled extinction values between 4000 and 7000 m for the scenario MIN4
300 match the observations quite well.

301 The ash cloud passed Leipzig on 16 April 2010 between 12 and 17 UT. A com-
302 parison of three lidar profiles with the modelled extinction values for the MIN4
303 scenario are given in Figure 5b. The model results show an ash cloud of simi-
304 lar maximum extinction values around 0.3 km^{-1} that decreases in height between
305 14 and 20 UT. Compared to the observations, the maximum extinction values are
306 lower and a time shift of about 4 hours delay in the modelled ash cloud was found.
307 Nevertheless the temporal development and the altitude of the ash cloud are cap-
308 tured quite well. Obviously, the model is not able to represent detailed vertical

309 structures and relatively thin aerosol layers due to a lack of vertical model res-
310 olution. This behaviour is typical for vertical extinction profiles simulated with
311 dynamical models. It has been reported in earlier publications about comparisons
312 of modelled aerosol vertical profiles to lidar observations (Guibert et al., 2005).
313 Unfortunately, simultaneous sun photometer observations were not available that
314 afternoon (see Fig. 4).

315 A comparison of the CMAQ model results to the lidar observations 2 days later
316 at the SIRTA site in Palaiseau/France (Haeffelin et al., 2005) clearly demonstrates
317 the difficulty to reproduce distinct aerosol layers (Fig. 6). The main observed
318 aerosol layer resides between 2000 and 2500 m asl and is about 500 m thick (see
319 also Colette et al. (2011)). Only some minor aerosol backscatter from higher al-
320 titudes was seen by the lidar. The model results, here given for the MIN2 and
321 MIN4 emission cases, on the other hand show a broad distribution of the volcanic
322 ash between 1000 and 6500 m asl with slightly enhanced values between 3000m
323 and 5000m. The modelled vertical ash distribution shows a similar behaviour over
324 Potenza/Italy on 20/21 April. Considering a delay of 4 -6 hours until the ash cloud
325 reaches the lidar station, the observed extinction values are in the same range as
326 the model results. However, the model shows a broad vertical distribution of the
327 ash in altitudes between 600m and 7000m asl while the lidar detects only low
328 aerosol extinction values above 4000 m and higher values close to ground.

329

330 *4.4. Ash concentrations*

331 In-situ observations of the volcanic ash concentrations by means of optical
332 particle counters (OPC) were performed with the DLR Falcon between 19 April
333 and 18 May 2010. Different size ranges between 4 nm and 800 μm were covered

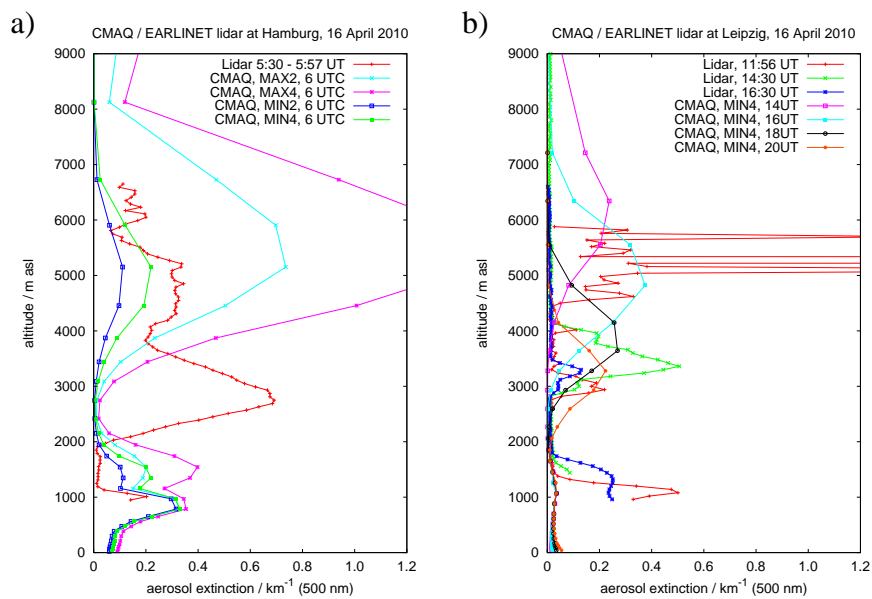


Figure 5: Comparison of CMAQ model results to vertical aerosol profiles detected with lidar instruments at a) Hamburg on 16 April 2010, b) Leipzig on 16 April 2010.

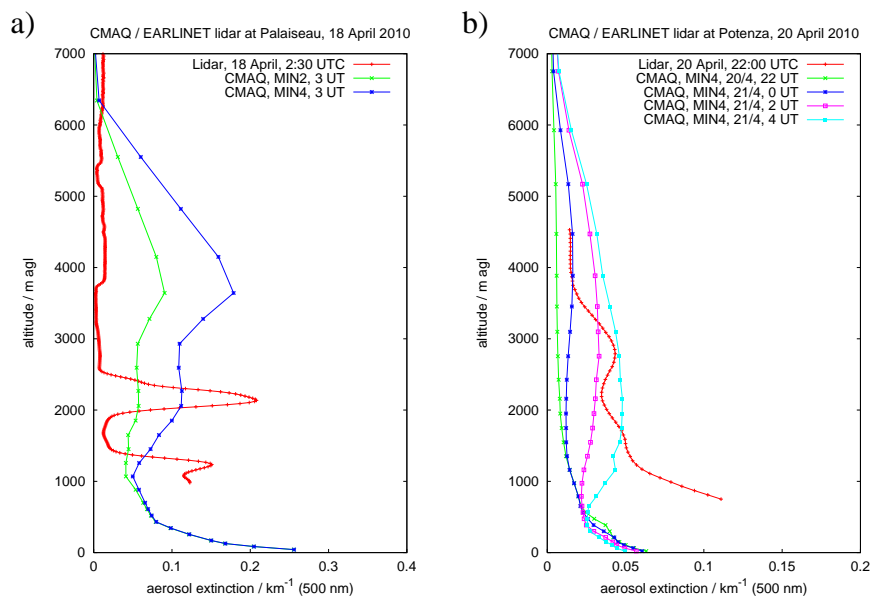


Figure 6: Comparison of CMAQ model results to vertical aerosol profiles detected with lidar instruments at a) Palaiseau on 18 April 2010 and b) Potenza on 20 April 2010.

334 by different instruments and measurement techniques. All details are given by
335 Schumann et al. (2010, 2011). The mass concentrations given for 12 locations
336 on 9 different days were compared to the model simulations. Fig. 7 exemplarily
337 shows four simulated concentration profiles together with the observations at the
338 time of the observations. The vertical error bars denote the given height range
339 in which the observations were performed while the horizontal error bars give
340 the uncertainty of the observations caused by the unknown imaginary part of the
341 refractive index of the volcanic ash. A low absorption of the ash particles repre-
342 sented by a small imaginary part of the refractive index leads to the lower con-
343 centration values and vice versa for a high imaginary part. The uncertainty of the
344 ash concentration was estimated to be a factor of two relative to the median values
345 plotted. The model results for the MIN2 emission case match the observations in
346 most cases very well. Typically the simulated concentrations are slightly higher
347 than the observations.

348 On 2 May (Fig. 7b) the aircraft flew close to the volcano in the upper part of the
349 ash plume. The model shows much higher concentrations in upper altitudes. This
350 is closely related to the assumptions about the emissions. On 2 May, the maxi-
351 mum emission height was estimated to be in 4.5 - 5 km asl. The vertical emission
352 profile with highest emissions in the maximum emission height (see the example
353 in Fig. 1c) is still visible in the concentration profile, as one would expect close
354 to the volcano. The aircraft observations suggest that the emissions were in lower
355 altitudes than prescribed for the model simulations.

356 The largest discrepancies considering all twelve cases were detected for the
357 flight over the North Sea on 17 May. Ash concentrations between approximately
358 100 and 300 $\mu\text{g}/\text{m}^3$ were observed in heights between 3.5 and 6 km while the

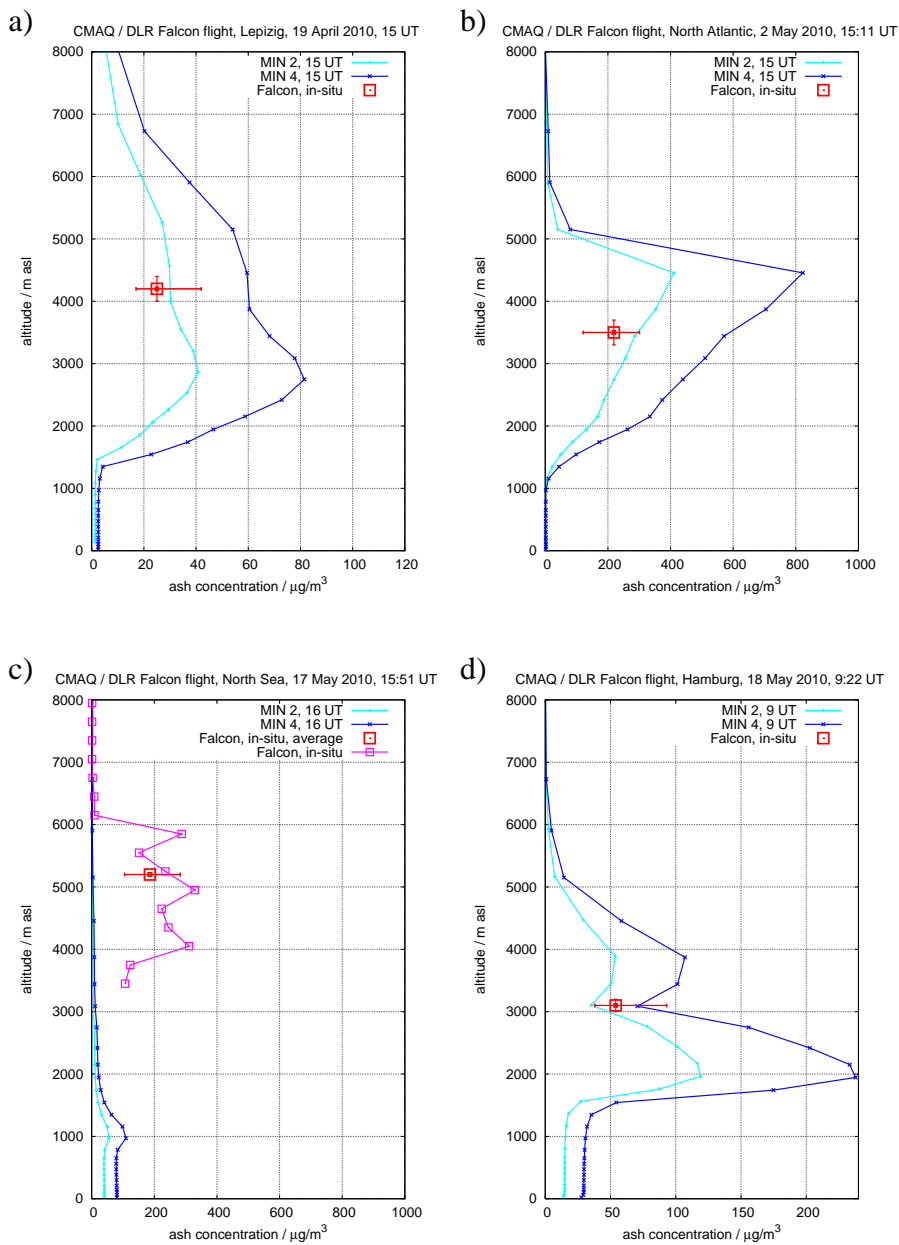


Figure 7: Comparison of CMAQ model results to in situ observation of the ash concentration aboard the DLR Falcon over a) Leipzig on 19 April 2010, b) the North Atlantic on 2 May 2010, c) North Sea on 17 May 2010, and d) Hamburg on 18 May 2010. Red squares denote the ash concentration under the assumption of a mean value (0.004) for the imaginary part of the refractive index. Horizontal error bars for the observations show the uncertainty caused by a variation of the imaginary part of the refractive index between 0 and 0.008. Vertical bars do not indicate an error but show the vertical variation in flight altitude during the observation period. For the observations on 17 May a vertical profile of the mass concentrations is plotted. The modelled values for the emission cases MIN2 and MIN4 are given at the hour of the in situ observations.

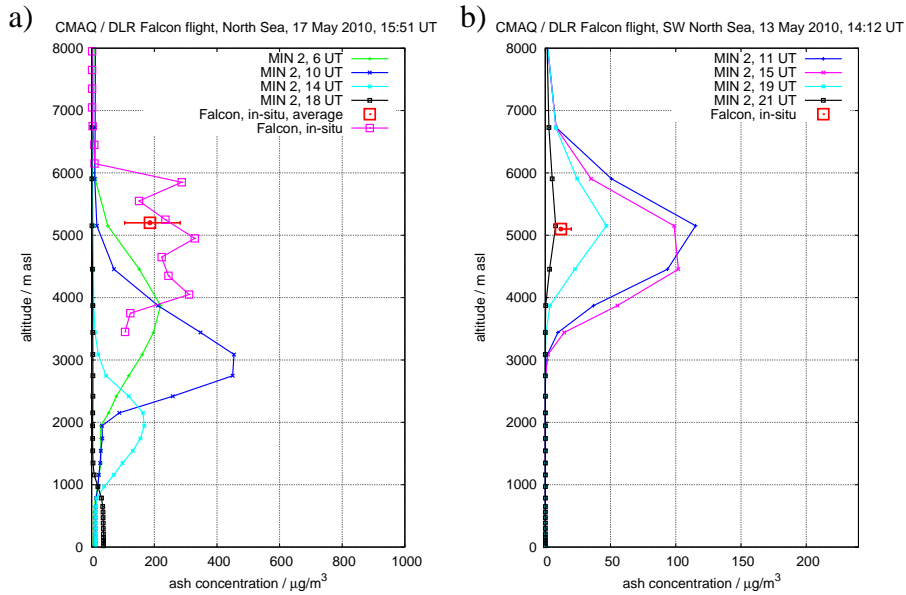


Figure 8: Comparison of CMAQ model results to in situ observation of the ash concentration aboard the DLR Falcon over the a) North Sea on 17 May 2010 and b) SW North Sea on 13 May 2010 considering a time shift in the passage of the ash cloud. Red squares denote the ash concentration under the assumption of a mean value (0.004) for the imaginary part of the refractive index. Horizontal error bars for the observations show the uncertainty caused by a variation of the imaginary part of the refractive index between 0 and 0.008. For the observations on 17 May a vertical profile of the mass concentrations is plotted. The modelled values for the emission case MIN2 are given.

Table 4: Comparison between modelled ash concentrations (in $\mu\text{g}/\text{m}^3$) for the MIN2 case and in situ observations aboard the DLR Falcon between 19 April and 18 May 2010. The range given for the observations represents different assumptions about the imaginary part of the refractive index. The range given for the model results represents the spread of model values in a time window of ± 2 hours around the observation time and in a vertical window of ± 500 m around the observation altitude.

Location	Latitude	Longitude	Time window /	altitude	Observations		Model results	
	North	East	UT	km	Mini	Maxi	Mini	Maxi
Leipzig	51.29	12.45	19.4., 15:08 - 15:15	4.2 \pm 0.2	17	42	28	32
Stuttgart	48.58	9.63	19.4., 17:19 - 17:21	3.8 \pm 0.1	13	29	35	76
Munich	47.89	11.09	19.4., 17:40 - 17:43	4.0 \pm 0.1	12	27	29	73
Skagerrak	58.05	8.57	22.4., 19:10 - 19:13	2.6 \pm 0.0	11	21	2	22
Baltic Sea	54.66	16.52	23.4., 12:37 - 12:38	2.7 \pm 0.0	13	19	6	14
North Atlantic	60.17	-15.17	2.5., 15:11 - 15:15	3.5 \pm 0.2	121	301	178	407
Munich	48.38	12.6	9.5., 14:56 - 15:01	4.1 \pm 0.2	10	16	8	29
SW North Sea	53.41	1.45	13.5., 14:12 - 14:15	5.1 \pm 0.0	11	20	72	114
NE England	54.76	-0.17	16.5., 14:08 - 14:16	6.1 \pm 0.4	19	40	20	44
North Sea	52.83	2.92	17.5., 15:51 - 16:58	5.2 \pm 1.6	105	283	1	5
Hamburg	53.17	9.12	18.5., 9:23 - 9:31	3.1 \pm 0.1	38	93	23	82
Stuttgart	48.87	9.97	18.5., 10:13 - 10:17	5.2 \pm 0.1	16	38	8	101

Table 5: Comparison between modelled ash concentrations (in $\mu\text{g}/\text{m}^3$) and in situ observations aboard the DLR Falcon considering a time shift in the model results of ± 10 hours and a height range of -1600 and +800 m for the observations on 17 May over the North Sea.

Location	Latitude	Longitude	Time window /	altitude	Observations		Model results	
	North	East	UT	km	Mini	Maxi	Mini	Maxi
SW North Sea	53.41	1.45	13.5., 14:12 - 14:15	5.1 ± 0.0	11	20	3	115
North Sea	52.83	2.92	17.5., 15:51 - 16:58	5.2 ± 1.6	105	283	0.1	394

359 simulations showed almost no ash in these heights at the same time (Fig. 7c).
360 The simulations show that a horizontally rather narrow cloud with high ash con-
361 centrations passed the western North Sea in the morning of 17 May. Schumann
362 et al. (2010) report travelling times of the ash cloud between 66 and 88 hours, de-
363 pending on altitude and the back-trajectory model used to derive the travel time.
364 The CMAQ simulations 4 and 8 hours before the flight show considerably higher
365 aerosol concentrations between 200 and $500 \mu\text{g}/\text{m}^3$ in altitudes between 2000m
366 and 6000m (Fig. 8a). However, the modelled ash cloud is in lower altitudes than
367 it has been observed. It is not clear what the reasons for this discrepancy are but
368 the modelled ash cloud was rather narrow and spatially inhomogeneous. As it
369 has been seen in the comparison on 2 May the emission height is also sensitive to
370 the vertical distribution of the ash. These uncertainties in the model results can
371 easily lead to the observed deviations to the measurements.
372 Table 4 summarizes the comparisons between the modelled ash concentrations
373 and the observations aboard the Falcon aircraft. The minimum and the maximum
374 values of the observed concentrations as given in Schumann et al. (2011) have
375 been compared to the range of model values for the MIN2 case in a height in-

376 terval of ± 500 m around the flight altitude and in a time window of ± 2 hours
377 around the observation time. In most cases the range of model values in this time-
378 height interval fits quite well with the observations. There were two exceptions,
379 the observations over the SW North Sea on 9 May and over the North Sea on 17
380 May. On 13 May a mismatch in time between the model and the observations ex-
381 plains the large differences. If a time window of ± 10 hours is considered instead
382 of ± 2 hours, the modelled values go down to $3 \mu\text{g}/\text{m}^3$ (see Table 5 and Fig. 8b).
383 If the same time window is considered on 17 May and the height interval is taken
384 from 3.6 to 6 km asl, the model captures also the high concentrations that were
385 observed.

386 Schumann et al. (2011) also report effective diameters of the ash particles that they
387 derived from their OPC measurements. Typical diameters of the particles were
388 rather small, between 0.2 and $2.1 \mu\text{m}$. Even observations in the North Atlantic
389 area close to the volcano showed small effective diameters of $1.8 \mu\text{m}$. These val-
390 ues are considerably smaller than the diameter of $6 \mu\text{m}$ that is assigned to coarse
391 mode aerosols in CMAQ. This could lead to a quicker sedimentation of the parti-
392 cles in the model, on the other hand particles of $5 \mu\text{m}$ size need about two weeks
393 to fall 1 km in the atmosphere by sedimentation (Jacobson, 1999). Thus, sedi-
394 mentation should be of minor importance in ash plumes that are on average 4 - 5
395 days old (Schumann et al., 2011) and the larger particle size in the model will not
396 affect the simulated concentrations in a significant way.

397 **5. Conclusions**

398 The development of the ash dispersion after the eruption of the Eyjafjal-
399 lajökull volcano on Iceland on 14 April 2010 has been simulated with the

400 three-dimensional Eulerian chemistry transport model CMAQ. Four different
401 emission cases were considered in order to take uncertainties in the emission
402 strength and emission height into account. The location and the extension of the
403 ash cloud agreed well with the forecasts that were provided during the eruption
404 phase by the Volcanic Ash Advisory Center (VAAC) in London. Comparisons of
405 the aerosol optical depth given by the model to observations within the Aerosol
406 Robotic Network (Aeronet) showed that the emission scenario MIN2 with lowest
407 emissions and low emission heights gives the best agreement. This could be
408 further verified by additional comparisons to vertical aerosol extinction profiles
409 derived within Earlinet and in-situ observations of the ash concentrations aboard
410 the DLR Falcon between 19 April and 18 May 2010. In some of the cases
411 the ash cloud travelled more slowly than in reality and the model showed only
412 good agreement to the observations if a time shift of a few hours was taken into
413 account. It was also obvious that the model could not reproduce distinct aerosol
414 layers of low vertical extension. The model tends to distribute the volcanic ash
415 more or less equally over many model layers in the free troposphere. This leads
416 to the fact that the extinction values in the MIN4 emission case agree better
417 with the lidar values than in the MIN2 case, but the aerosol optical depth is then
418 overestimated due to the wider vertical spread of the ash cloud. On the one hand
419 this might be improved if more layers and therefore a better vertical resolution
420 would be taken into account in higher altitudes. On the other hand effects of
421 the aerosol layer on the thermal stratification, e.g. due to absorption of radiation
422 within the aerosol layer are not taken into account in the model.

423

424 **Acknowledgements**

425 US EPA is gratefully acknowledged for the use of CMAQ. We thank the PIs
426 and their staff for establishing and maintaining the 11 sites at Belsk, Cabauw,
427 Chilbolton, Hamburg, Helgoland, Leipzig, Lille, Minsk, Munich, Palaiseau and
428 Wytham Woods used in this investigation.

429

430 **References**

431 Ansmann, A., Riebesell, M., Wandinger, U., Weitkamp, C., Voss, E., Lahmann,
432 W., Michaelis, W., 1992. Combined Raman Elastic-Backscatter LIDAR for Ver-
433 tical Profiling of Moisture, Aerosol Extinction, Backscatter, and LIDAR Ratio.
434 *Applied Physics B* 55, 18–28.

435 Ansmann, A., Tesche, M., Gross, S., Freudenthaler, V., Seifert, P., Hiebsch, A.,
436 Schmidt, J., Wandinger, U., Mattis, I., Müller, D., Wiegner, M., 2010. The
437 16 April 2010 major volcanic ash plume over central Europe: EARLINET li-
438 dar and AERONET photometer observations at Leipzig and Munich, Germany.
439 *Geophysical Research Letters* 37.

440 Bieser, J., Aulinger, A., Matthias, V., Quante, M., Builtjes, P., 2010. SMOKE for
441 Europe - adaptation, modification and evaluation of a comprehensive emission
442 model for Europe. *Geoscientific Model Development* 3 (3), 949–1007.

443 Bösenberg, J., Matthias, V., Amodeo, A., Amoiridis, V., Ansmann, A., Baldasano,
444 J. M., Balin, I., Balis, D., Böckmann, C., Boselli, A., Carlsson, G., Chaikovsky,
445 A., Chourdakis, G., Comerón, A., Tomasi, F. D., Eixmann, R., Freudenthaler,
446 V., Giehl, H., Grigorov, I., Hågård, A., Iarlori, M., Kirsche, A., Kolarov, G.,
447 Komguem, L., Kreipl, S., Kumpf, W., Larchevêque, G., Linné, H., Matthey, R.,

448 Mattis, I., Mekler, A., Mironova, I., Mitev, V., Mona, L., Müller, D., Music, S.,
449 Nickovic, S., Pandolfi, M., Papayannis, A., Pappalardo, G., Pelon, J., Pérez, C.,
450 Perrone, R. M., Persson, R., Resendes, D. P., Rizi, V., Rocadenbosch, F., Ro-
451 drigues, J. A., Sauvage, L., Schneidenbach, L., Schumacher, R., Shcherbakov,
452 V., Simeonov, V., Sobolewski, P., Spinelli, N., Stachlewska, I., Stoyanov, D.,
453 Trickl, T., Tsaknakis, G., Vaughan, G., Wandinger, U., Wang, X., Wiegner, M.,
454 Zavrtnik, M., Zerefos, C., 2003. A European Aerosol Research Lidar Network
455 to Establish an Aerosol Climatology. MPI-Report 348, Max-Planck-Institut für
456 Meteorologie, Hamburg.

457 Colette, A., Favez, O., Meleux, F., Chiappini, L., Haeffelin, M., Morille, Y., Mal-
458 herbe, L., Papin, A., Bessagnet, B., Menut, L., Leoz, E., Roul, L., Feb. 2011.
459 Assessing in near real time the impact of the April 2010 Eyjafjallajökull ash
460 plume on air quality. *Atmospheric Environment* 45 (5), 1217–1221.

461 Eck, T. F., Holben, B. N., Reid, J. S., Dubovik, O., Smirnov, A., O’Neill, N. T.,
462 Slutsker, I., Kinne, S., 1999. Wavelength dependence of the optical depth of
463 biomass burning, urban and desert dust aerosols. *J. Geophys. Res.* 104, 31333 –
464 31350.

465 Fernald, F. G., Herman, B. M., Reagan, J. A., 1972. Determination of aerosol
466 height distributions by lidar. *Journal of Applied Meteorology* 11, 482–489.

467 Gery, M. W., Whitten, G. Z., Killus, J. P., Dodge, M. C., 1989. A photochemical
468 kinetics mechanism for urban and regional scale computer modeling. *J. Geo-
469 phys. Res.* 94, 12925 – 12956.

470 Guenther, A., Hewitt, C. N., Erickson, D., Fall, R., Greon, C., Graedel, T., Harley,

471 P., Klinger, L., Lerdau, M., McKay, W. A., Pierce, T., Scholes, B., Steinbrecher,
472 R., Tallamraju, R., Taylor, J., Zimmerman, P., 1995. A Global Model of Nat-
473 ural Volatile Organic Compound Emissions. *Journal of Geophysical Research-*
474 *Atmospheres* 100 (D5), 8873–8892.

475 Guibert, S., Matthias, V., Schulz, M., Bosenberge, J., Eixmann, R., Mattis, I., Pap-
476 palardo, G., Perroneg, M. R., Spinelli, N., Vaughan, G., 2005. The vertical dis-
477 tribution of aerosol over Europe - synthesis of one year of EARLINET aerosol
478 lidar measurements and aerosol transport modeling with LMDzT-INCA. *Atmo-*
479 *spheric Environment* 39 (16), 2933–2943.

480 Haeffelin, M., Barthes, L., Bock, O., Boitel, C., Bony, S., Bouniol, D., Chep-
481 fer, H., Chiriaco, M., Cuesta, J., Delanoe, J., Drobinski, P., Dufresne, J. L.,
482 Flamant, C., Grall, M., Hodzic, A., Hourdin, F., Lapouge, R., Lemaitre, Y.,
483 Mathieu, A., Morille, Y., Naud, C., Noel, V., O’Hirok, W., Pelon, J., Pietras, C.,
484 Protat, A., Romand, B., Scialom, G., Vautard, R., 2005. SARTA, a ground-based
485 atmospheric observatory for cloud and aerosol research. *Annales Geophysicae*
486 23 (2), 253–275.

487 Holben, B. N., Eck, T. F., Slutsker, I., Tanré, D., Buis, J. P., Setzer, A., Vermote, E.,
488 Reagan, J. A., Kaufman, Y. J., Nakajima, T., Lavenue, F., Jankowiak, I., Smirnov,
489 A., 1998. AERONET- A Federated Instrument Network and Data Archive for
490 Aerosol Characterization. *Remote Sens. Environment* 66, 1–16.

491 Holben, B. N., Tanré, D., Smirnov, A., Eck, T. F., Slutsker, I., Abuhassan, N.,
492 Newcomb, W., Schafer, J., Chatenet, B., Lavenue, F., Kaufman, Y. J., Van
493 de Castle, J., Setzer, A., Markham, B., Clark, D., Frouin, R., Halthore, R.,
494 Karnieli, A., O’Neill, N. T., Pietras, C., Pinker, R. T., Voss, K., Zibordi, G.,

- 495 2001. An emerging ground-based aerosol climatology: Aerosol Optical Depth
496 from AERONET. *J. Geophys. Res.* 106, 12 067 – 12097.
- 497 Jacobson, M. Z., 1999. *Fundamentals of Atmospheric Modelling*. Cambridge Uni-
498 versity Press, Cambridge, UK.
- 499 Kalnay, E., Kanamitsu, M., Kistler, R., Collins, W., Deaven, D., Gandin, L.,
500 Iredell, M., Saha, S., White, G., Woollen, J., Zhu, Y., Chelliah, M., Ebisuzaki,
501 W., Higgins, W., Janowiak, J., Mo, K. C., Ropelewski, C., Wang, J., Leet-
502 maa, A., Reynolds, R., Jenne, R., Joseph, D., Mar. 1996. The NCEP/NCAR
503 40-year reanalysis project. *Bulletin of the American Meteorological Society*
504 77 (3), 437–471.
- 505 Langmann, B., Folch, A., Hensch, M., Matthias, V., 2011. Volcanic ash over Eu-
506 rope during the eruption of Eyjafjallajökull on Iceland, April-May 2010. *Atmo-
507 spheric Environment* this issue.
- 508 Malm, W. C., Sisler, J. F., Huffman, D., Eldred, R. A., Cahill, T. A., 1994. Spatial
509 and seasonal trends in particle concentration and optical extinction in the United
510 States. *Journal of Geophysical Research* 99 (D1), 1347 – 1370.
- 511 Mastin, L. G., Guffanti, M., Servranckx, R., Webley, P., Barsotti, S., Dean, K., Du-
512 rant, A., Ewert, J. W., Neri, A., Rose, W. I., Schneider, D., Siebert, L., Stunder,
513 B., Swanson, G., Tupper, A., Volentik, A., Waythomas, C. F., 2009. A multi-
514 disciplinary effort to assign realistic source parameters to models of volcanic
515 ash-cloud transport and dispersion during eruptions. *Journal of Volcanology
516 and Geothermal Research* 186 (1-2), 10–21.

- 517 Matthias, V., 2008. The aerosol distribution in Europe derived with the Commu-
518 nity Multiscale Air Quality (CMAQ) model: Comparison to near surface in
519 situ and sunphotometer measurements. *Atmospheric Chemistry and Physics* 8,
520 5077–5097.
- 521 Matthias, V., Aulinger, A., Quante, M., 2009. CMAQ simulations of the
522 benzo(a)pyrene distribution over Europe for 2000 and 2001. *Atmospheric En-
523 vironment* 43, 4078–4086, doi:10.1016/j.atmosenv.2009.04.058.
- 524 Rockel, B., Will, A., Hense, A., 2008. The Regional Climate Model COSMO-
525 CLM(CCLM). *Meteorologische Zeitschrift* 17 (4), 347–348.
- 526 Schumann, U., Weinzierl, B., Reitebuch, O., Schlager, H., Minikin, A., Forster,
527 C., Baumann, R., Sailer, T., Graf, K., Mannstein, H., Voigt, C., Rahm, S.,
528 Simmet, R., Scheibe, M., Lichtenstern, M., Stock, P., Rüba, H., Schäuble, D.,
529 Tafferner, A., Rautenhaus, M., Gerz, T., Ziereis, H., Krautstrunk, M., Mallaun,
530 C., Gayet, J.-F., Lieke, K., Kandler, K., Ebert, M., Weinbruch, S., Stohl, A.,
531 Gasteiger, J., Olafsson, H., Sturm, K., 2010. Airborne observations of the Ey-
532 jafjalla volcano ash cloud over Europe during air space closure in April and
533 May 2010. *Atmospheric Chemistry and Physics Discussions* 10 (9), 22131–
534 22218.
- 535 Schumann, U., Weinzierl, B., Reitebuch, O., Schlager, H., Minikin, A., Forster,
536 C., Baumann, R., Sailer, T., Graf, K., Mannstein, H., Voigt, C., Rahm, S.,
537 Simmet, R., Scheibe, M., Lichtenstern, M., Stock, P., Rüba, H., Schäuble, D.,
538 Tafferner, A., Rautenhaus, M., Gerz, T., Ziereis, H., Krautstrunk, M., Mallaun,
539 C., Gayet, J.-F., Lieke, K., Kandler, K., Ebert, M., Weinbruch, S., Stohl, A.,

540 Gasteiger, J., Olafsson, H., Sturm, K., 2011. Airborne observations of the Ey-
541 jafjalla volcano ash cloud over Europe during air space closure in April and
542 May 2010. Atmospheric Chemistry and Physics submitted.

543 Witham, C. S., Hort, M. C., Potts, R., Servranx, R., Husson, P., Bonnardot,
544 F., 2007. Comparison of VAAC atmospheric dispersion models using the 1
545 November 2004 Grimsvötn eruption. Meteorol. Appl. 14, 27–38.